23. Tokuno, H., Hatanaka, N., Takada, M. & Nambu, A. B-mode and color Doppler ultrasound imaging for localization of microelectrode in monkey brain. *Neurosci. Res.* **36,** 335–338 (2000).

Supplementary Information is available on *Nature*'s World-Wide Web site (http://www.nature.com) or as paper copy from the London editorial office of *Nature*.

Acknowledgements

We thank M. Kurama, Y. Takahashi and S. Hoffman for technical assistance. This work was supported by the Japan Society for the Promotion of Science (E.H.), by the Ministry of Education, Science, and Culture of Japan, and by the Japan Science and Technology Corporation (J.T.).

Correspondence and requests for materials should be addressed to J.T. (e-mail: tanjij@mail.cc.tohoku.ac.jp).

MOD-1 is a serotonin-gated chloride channel that modulates locomotory behaviour in *C. elegans*

Rajesh Ranganathan*, Stephen C. Cannon† & H. Robert Horvitz*

** Howard Hughes Medical Institute, Department of Biology, Room 68-425, Massachusetts Institute of Technology, 77 Massachusetts Avenue, Cambridge, Massachusetts 02139, USA*
† Department of Neurobiology, Harvard Medical School, Boston, Massachusetts 02115, and Department of Neurology, Massachusetts General Hospital, Boston, Massachusetts 02114, USA

The neurotransmitter and neuromodulator serotonin (5-HT) functions by binding either to metabotropic G-protein-coupled receptors (for example, 5-HT$_1$, 5-HT$_2$, 5-HT$_4$ to 5-HT$_7$), which mediate 'slow' modulatory responses through numerous second messenger pathways[1], or to the ionotropic 5-HT$_3$ receptor, a non-selective cation channel that mediates 'fast' membrane depolarizations[2]. Here we report that the gene *mod-1* (for modulation of locomotion defective) from the nematode *Caenorhabditis elegans* encodes a new type of ionotropic 5-HT receptor, a 5-HT-gated chloride channel. The predicted MOD-1 protein is similar to members of the nicotinic acetylcholine receptor family of ligand-gated ion channels, in particular to GABA (γ-aminobutyric acid)- and glycine-gated chloride channels. The MOD-1 channel has distinctive ion selectivity and pharmacological properties. The reversal potential of the MOD-1 channel is dependent on the concentration of chloride ions but not of cations. The MOD-1 channel is not blocked by calcium ions or 5-HT$_{3a}$-specific antagonists but is inhibited by the metabotropic 5-HT receptor antagonists mianserin and methiothepin. *mod-1* mutant animals are defective in a 5-HT-mediated experience-dependent behaviour[3] and are resistant to exogenous 5-HT, confirming that MOD-1 functions as a 5-HT receptor *in vivo*.

The locomotory rate of a well-fed *C. elegans* hermaphrodite slows when it encounters bacteria (the basal slowing response[3]); this slowing response is enhanced markedly if the animal has been deprived of food for 30 min before the encounter (the enhanced slowing response[3] (Fig. 1a). In a genetic screen for mutants defective in the enhanced slowing response, we identified the gene *mod-1*, which is defined by the mutation *n3034* (ref. 3). On Petri dishes with bacteria, the locomotory rate of food-deprived *mod-1* mutants is significantly faster than that of the wild type (strain N2) (Fig. 1a, grey bars). On dishes without bacteria, the locomotory rate of food-deprived *mod-1* mutants is not different from that of food-deprived wild-type animals (Fig. 1a, grey bars). Well-fed *mod-1* mutants show no defect in their basal slowing response to bacteria (Fig. 1a, black bars).

The swimming behaviour of *mod-1(n3034)* mutants was not affected by exogenous 5-HT treatment, whereas exogenous 5-HT inhibits wild-type *C. elegans* locomotion[4]; and this phenotype was semi-dominant in a time-dependent manner (Fig. 1b), which aided our cloning of the *mod-1* gene (see below). This 5-HT resistance of *mod-1* mutants is consistent with the finding that the enhanced slowing response is mediated by 5-HT signalling[3] and the hypothesis that *mod-1* mutants are deficient in 5-HT signalling[3].

We used standard genetic three-factor mapping and scored the 5-HT resistance of *mod-1* mutants to locate *mod-1* to a ~400 kilobase (kb) region on chromosome V. Cosmid C38E12 from this region rescued the recessive aspect of the Mod-1 mutant phenotype of 5-HT resistance, as assayed by the response to exogenous 5-HT after 5 min (Fig. 1c). We narrowed the rescuing activity to a 5.5-kb fragment (Fig. 1c) containing a single predicted gene[5]. We isolated several complementary DNAs with SL1 *trans*-spliced leaders, located at the 5′ ends of many *C. elegans* transcripts[6], and determined the complete *mod-1* transcription unit (Fig. 2a). Genomic subclones lacking all or part of this transcription unit did not rescue the Mod-1 phenotype of 5-HT resistance (Fig. 1c).

MOD-1 is similar to members of the nicotinic acetylcholine receptor (nAChR) family of ligand-gated ion channels, in particular to GABA- and glycine-gated chloride channels (Fig. 2b). We found a single-base transition mutation in the *mod-1* coding sequence in *n3034* mutants (Fig. 2b, c), in which Ala 281 (codon GCT) is changed to valine (GTT) in the predicted M2 transmembrane domain of the MOD-1 protein. M2 is thought to be critical for channel function. We used site-directed mutagenesis to introduce this C-to-T (A281V) mutation into the 5.5-kb minimal rescuing

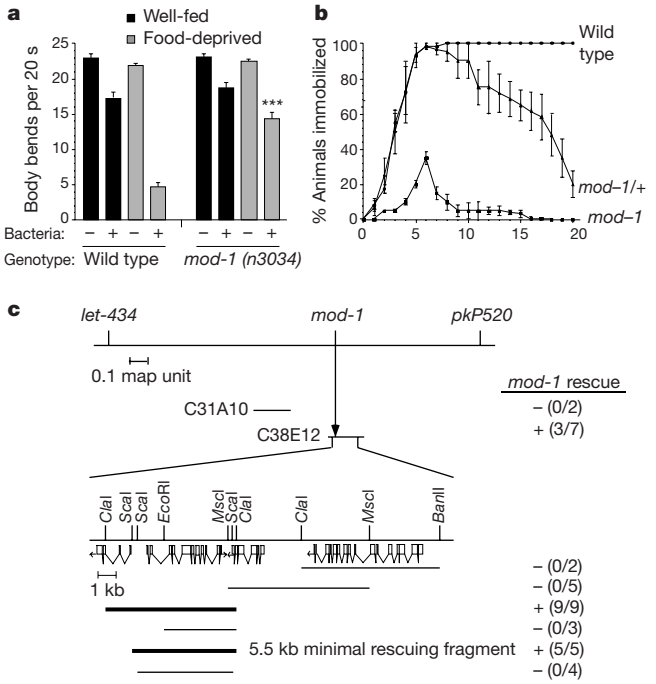

Figure 1 Phenotypic characterization and cloning of *mod-1*. **a**, *mod-1(n3034)* mutants were defective in the enhanced slowing locomotory response exhibited by food-deprived wild-type animals[3]. Ten trials were performed for each genotype. Error bars represent s.e.m.; asterisks, $P < 0.0001$, Student's *t*-test. **b**, Time course of response to 33 mM 5-HT. The resistance to exogenous 5-HT of *mod-1(n3034)* mutants was recessive at early time points and was semi-dominant at later time points. **c**, Genetic and physical maps of the relevant region of linkage group V. Cosmid C38E12 and subclones shown in bold rescued *mod-1*; +, rescue; –, no rescue. Numbers in parentheses represent the fraction of transgenic lines tested that rescued *mod-1*.

fragment and generated transgenic animals carrying extrachromosomal arrays of this fragment, Ex[MOD-1(A281V)]. These transgenic animals displayed resistance to exogenous 5-HT (Fig. 3a), confirming that the A281V mutation in MOD-1 is sufficient to cause 5-HT resistance.

To determine the effect of eliminating *mod-1* function, we analysed two deletion alleles of *mod-1*, *nr2043* (ref. 7) and *ok103* (Fig. 2a), obtained by screening libraries of mutagenized animals for large deletions in the *mod-1* genomic locus[8]. Both *mod-1(nr2043)* and *mod-1(ok103)* mutants, when deprived of food, were defective in the enhanced slowing response (Fig. 3b), whereas neither was defective in the basal slowing response (data not shown). Both deletion mutants were resistant to exogenous 5-HT (Fig. 3a). The 5-HT resistance caused by the two deletion alleles was completely recessive throughout the 20-min time course (Fig. 3a; and data not shown), consistent with our observation that animals heterozygous for large chromosomal deficiencies that uncover the *mod-1* genomic locus are not 5-HT-resistant (data not shown). The molecular nature of the *mod-1(nr2043)* and *mod-1(ok103)* mutations suggests that they are null alleles. As null alleles confer the same phenotype as Ex[MOD-1(A281V)], *mod-1(n3034)* is likely to be a dominant-negative allele.

MOD-1 protein is predicted to contain a large extracellular amino terminus with two cysteine residues separated by 13 amino acids, a region that is conserved in the nAChR family and that may have a role in subunit assembly and insertion into the membrane[9] (Fig. 2b). There are four predicted transmembrane regions (M1–M4) and a large cytoplasmic domain between M3 and M4 (Fig. 2b). The M2 domain may participate in forming the pore of the channel after these nAChR family members assemble as multimeric complexes in the cell membrane[10]. In other family members, the residues in and around the M2 domain help establish ion selectivity[10]. We could not confidently predict the ion selectivity of the MOD-1 channel from sequence comparisons.

We examined the ability of MOD-1 to form functional channels in voltage-clamped *Xenopus laevis* oocytes. Oocytes injected with *mod-1* complementary RNA and voltage-clamped at −70 mV responded to 1 μM 5-HT with a large, rapidly developing, non-oscillatory inward current (Fig. 4a), whereas control oocytes injected with water showed no such response to application of any agonist (data not shown). Even 1,000 μM glycine, acetylcholine, GABA, glutamate or histamine—neurotransmitters that can activate ion channels[11–13]—did not elicit an inward current in *mod-1*-injected oocytes (Fig. 4a; and data not shown). Similarly, 10 μM ivermectin failed to elicit any current in MOD-1-injected oocytes (data not shown). Ivermectin, an anthelmintic drug that activates glutamate-gated chloride channels in nematodes[14], can activate a rat α1β2γ2S-GABA-gated chloride channel[15] and enhances acetylcholine-evoked responses of the human nAChRα7 receptor[16]. Dopamine, octopamine or tyramine did not elicit MOD-1-dependent inward currents at 100 μM, but elicited small responses at millimolar concentrations (data not shown). *mod-1* mutants did not have defects associated with impaired dopamine or octopamine signalling (ref. 3; and M. Alkema, R.R. and H.R.H., unpublished observations). We conclude that 5-HT is most likely to be the native ligand for the MOD-1 channel. 5-HT dose–response experiments using oocytes showed that the MOD-1 channel has an effector concentration for half-maximal response (EC_{50}) of 1.0 ± 0.1 μM (Fig. 4b), which is lower than that of the human 5-HT_{3a} channel

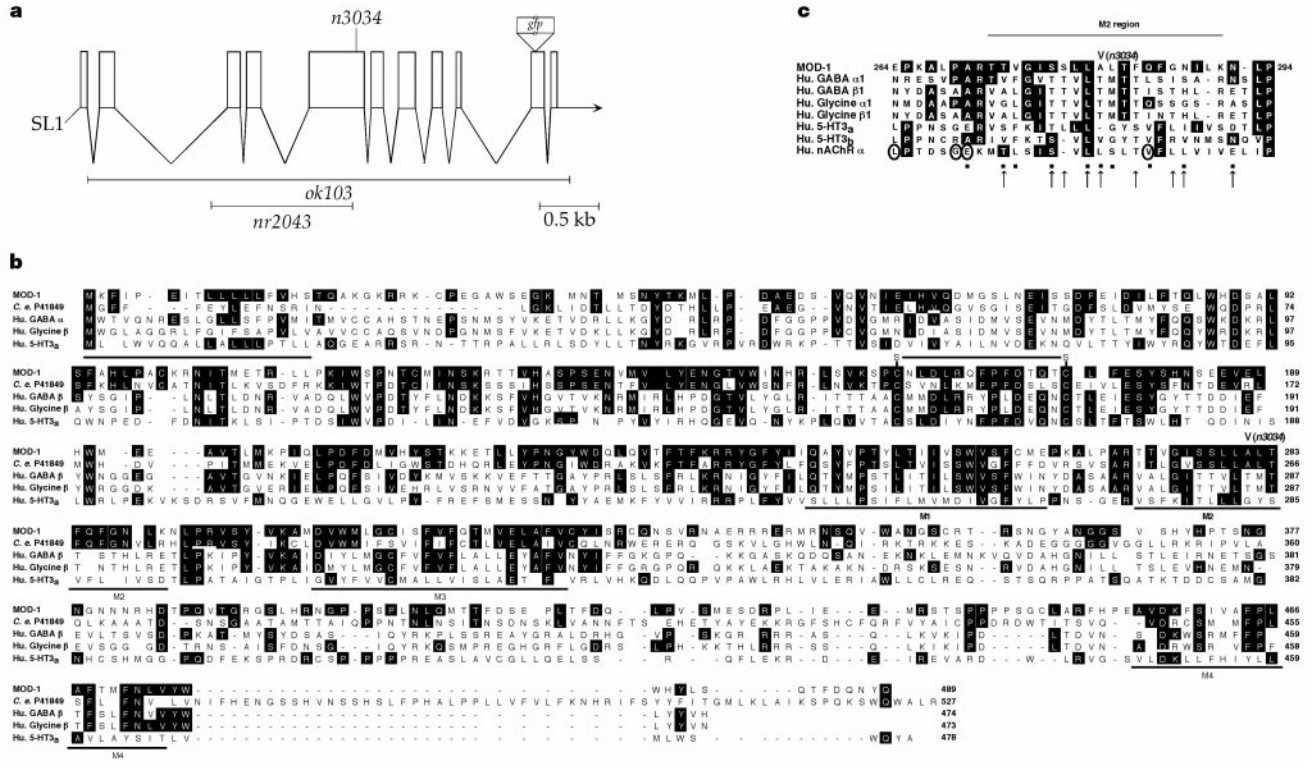

Figure 2 Sequence analysis of *mod-1*. **a**, *mod-1* intron–exon structure. Open boxes, coding regions; lines, untranslated regions; arrow, direction of transcription; *SL1*, *SL1 trans*-spliced leader. The *ok103* and *nr2043* deletions are depicted (see Supplementary Information), and the positions of the *n3034* mutation and insertion site of the *gfp* gene are indicated. **b**, Amino-acid sequence alignment of MOD-1 with a *C. elegans* predicted protein (P41849) that is most similar to MOD-1, human $GABA_A$ receptor β1 subunit (A40336), human glycine receptor β subunit (NP_000815.1), and the human 5-$HT3_a$ subunit (BAA08387). The putative signal sequence and M1–M4 regions are underlined, and the Cys–Cys loop is indicated (S–S). Amino acids conserved between MOD-1 and at least one other protein are shown in black boxes. *mod-1(n3034)* is a C-to-T mutation resulting in an A281V substitution. **c**, Alignment of the M2 regions from MOD-1, human $GABA_A$ α1 subunit (A60652), human $GABA_A$ β1 subunit, human glycine α1 subunit (NP_000162), human glycine β1 subunit, 5-$HT3_a$, 5-$HT3_b$ (AF080582) and human nAChR α-subunit (P02708). Dots, residues that probably face the pore in the nAChR[10]; arrows, residues that probably face the pore in the $GABA_A$ receptor[10]; circles, residues conserved in cation channels that are not conserved in MOD-1.

($2.9 \pm 0.1\ \mu M$)[17]. Unlike the 5-HT_{3a} channel[2], the MOD-1 channel was not blocked by calcium (Fig. 4c). High concentrations of granisetron (Fig. 4d) and ondansetron (data not shown), both of which are potent antagonists of the 5-HT_{3a} channel[18], did not affect the action of 5-HT on MOD-1 channels.

Pretreatment of wild-type *C. elegans* with mianserin or methiothepin—5-HT receptor antagonists—prevents food-deprived animals from exhibiting the wild-type enhanced slowing response[3]. Therefore, even though both compounds have so far been considered to be primarily antagonists of metabotropic 5-HT

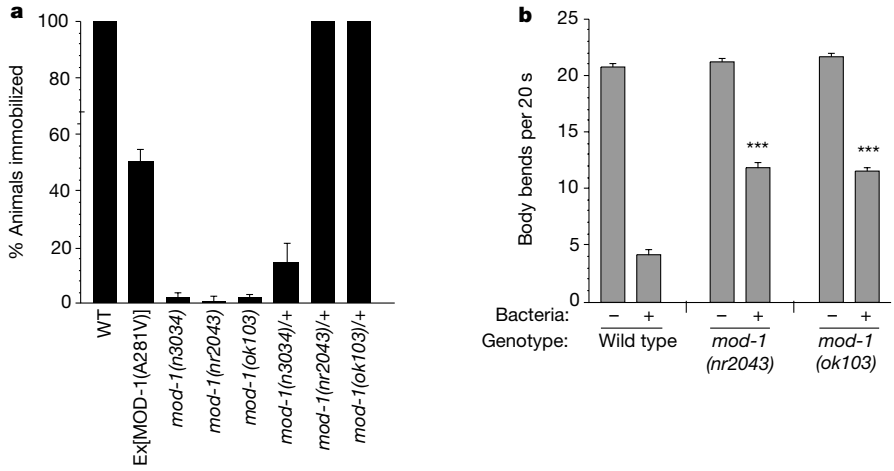

Figure 3 *mod-1* deletion alleles caused 5-HT resistance and defects in the enhanced slowing response. **a**, 5-HT sensitivity, scored after 20 min in 33 mM 5-HT. Ex[MOD-1(A281V)] is an extrachromosomal array containing the wild-type *lin-15* gene and the *mod-1* genomic locus encoding the A281V mutant form of the MOD-1 protein. Control transgenic lines with extrachromosomal arrays containing wild-type *lin-15* and *mod-1* genes were not resistant to 5-HT (data not shown). **b**, *mod-1* deletion mutants were defective in the enhanced slowing response. Ten trials were performed for each genotype. Error bars represent s.e.m.; asterisks, $P < 0.0001$, Student's *t*-test.

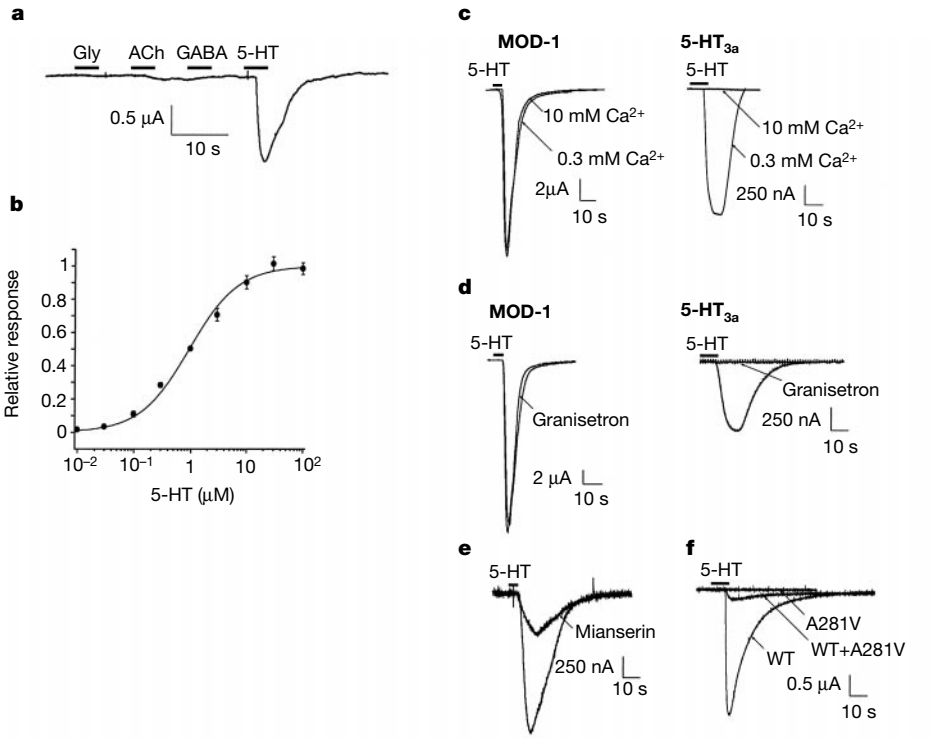

Figure 4 MOD-1 is a 5-HT-gated ion channel distinct from the 5-HT_{3a} channel. Recordings were from *Xenopus* oocytes voltage clamped at −70 mV in standard ND-96 bath solution, except in **c** where the Ca^{2+} concentrations were varied. Bars, durations of agonist application. **a**, 1 μM 5-HT elicited a rapidly developing inward current from oocytes injected with *mod-1* cRNA. A representative trace is shown from an oocyte treated with 1 mM Gly, ACh and GABA, and 1 μM 5-HT in ND-96 ($n = 5$). The order of agonist application was not important (data not shown). **b**, 5-HT dose response curve; $EC_{50} = 1.0 \pm 0.1\ \mu M$; $n \geq 4$ for each concentration; error bars represent s.e.m. **c**, Extracellular calcium did not block the MOD-1 channel. Representative traces are shown from oocytes injected with *mod-1* ($n = 3$) or 5-$HT3_a$ ($n = 2$) cRNA and treated with 1 μM (*mod-1*) or 10 μM (5-$HT3_a$) 5-HT. **d**, The 5-HT_{3a}-specific blocker granisetron did not block MOD-1. Representative traces are shown from oocytes injected with *mod-1* or 5-$HT3_a$ cRNA ($n = 2$ for each) and treated with 1 μM (*mod-1*) or 10 μM (5-$HT3_a$) 5-HT with or without 130 μM granisetron. **e**, Mianserin blocked the MOD-1 channel. Representative traces are shown from *mod-1*-injected oocytes ($n = 5$) treated with 0.5 μM 5-HT with or without 50 μM mianserin. **f**, The MOD-1(A281V) mutant channel has a dominant-negative effect. Representative traces are shown from oocytes injected with wild-type *mod-1* cRNA (WT), *mod-1* cRNA encoding the A281V mutant protein (A281V), or four parts wild type to one part A281V (WT+A281V) ($n \geq 4$ for each class). Wild-type oocytes were treated with 1 μM 5-HT; A281V and WT+A281V oocytes were treated with 10 μM 5-HT; 1 μM 5-HT did not elicit any response from either A281V or WT+A281V oocytes.

receptors[19,20], we tested their effects on MOD-1 in oocytes. The MOD-1 channel was inhibited by mianserin and methiothepin, with inhibition constants (K_i) of ~19 μM and ~32 μM, respectively (Fig. 4e; and data not shown). Pretreatment of *mod-1* mutants with mianserin or methiothepin did not further affect the defective enhanced slowing response of these animals (data not shown). Manserin and methiothepin may therefore interfere with the enhanced slowing response of *C. elegans* by antagonizing the MOD-1 5-HT-gated channel.

We tested the effect on channel function of the MOD-1(A281V) substitution in the *mod-1(n3034)* mutant. When antisense RNA (cRNA) encoding MOD-1(A281V) was injected into oocytes, no 5-HT-gated responses were observed (Fig. 4f). When the mutant cRNA was co-injected with roughly a fourfold excess of wild-type *mod-1* cRNA, the magnitude of the current through the wild-type channels was markedly reduced compared with that of oocytes that had been injected with the same amount of only the wild-type cRNA (Fig. 4f). These findings indicate that the MOD-1 channel may be multimeric, and that mutant MOD-1(A281V) channel subunits may interfere in a dominant manner with the function of wild-type MOD-1 channel subunits. Alternatively, MOD-1(A281V) channel subunits might interfere with wild-type MOD-1 channel function in a nonspecific manner, for example, by affecting assembly, transport or stability of all membrane proteins. Our genetic data support this hypothesis in that *mod-1(n3034)* encodes a dominant-negative form of MOD-1.

Current–voltage (I–V) relationships showed that the 5-HT-dependent current from MOD-1-expressing oocytes reverses direction (in ND-96 bath solution) near −20 mV (data not shown), significantly different from the near 0 mV reversal potential of the 5-HT_{3a} non-selective cation channel (ref. 2; and our unpublished data). The chloride reversal potential (E_{Cl}) in *Xenopus* oocytes is roughly −20 mV (ref. 21), consistent with the hypothesis that MOD-1 is a chloride channel. Moreover, when external sodium chloride was replaced with choline chloride, there was no change in the MOD-1 reversal potential (data not shown), indicating that sodium was not the primary charge carrier through the MOD-1 channel.

We directly tested whether chloride-ion concentration affected the reversal potential of the MOD-1 channel. To avoid activities of chloride channels endogenous to the *Xenopus* oocyte[21] and to be able to manipulate the concentrations of ions on both sides of the membrane, we conducted these experiments using human embryonic kidney 293 (HEK293) cells transiently transfected with a *mod-1* cDNA. We found that the peak I–V relationship showed no evidence of rectification (Fig. 5a), indicating that there was no voltage-dependent block by divalent cations or small organic molecules. Mock-transfected control HEK293 cells did not have any 5-HT-gated responses (data not shown). We also found that a 10-fold change in external chloride concentration shifted the reversal potential by 53 mV (Fig. 5b), in good agreement with the theoretical shift of 58 mV predicted by the Nernst equation if the MOD-1 channel were perfectly selective for chloride ions. Thus, MOD-1 is a 5-HT-gated chloride channel.

As the M2 region of the MOD-1 channel is similar to those of GABA- and glycine-gated chloride channels (Fig. 2c) and these

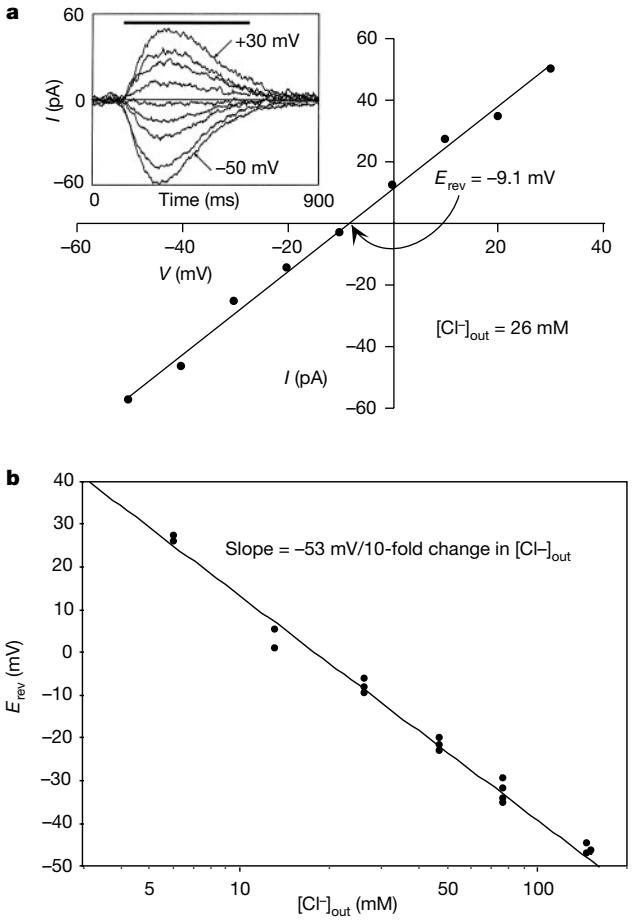

Figure 5 MOD-1 is a 5-HT-gated chloride channel. Whole-cell recordings from HEK293 cells transfected with a *mod-1* cDNA. **a**, The I–V relationship of the maximal responses from a representative cell when the external solution contained 120 mM sodium gluconate and 20 mM NaCl, resulting in $[Cl^-]_{out}$ = 26 mM, $[Na^+]_{in}$ = 0, and $[Cl^-]_{in}$ = 12 mM (see Methods for complete salt compositions). E_{rev} = −9.1 mV. Inset, raw traces for this cell at each of the nine voltage steps from −50 mV to +30 mV. Bar, duration of 100 nM 5-HT application. **b**, The reversal potential varied linearly with log$[Cl^-]_{out}$. Each data point represents E_{rev} of a single cell at one particular $[Cl^-]_{out}$ as in **a**.

channels are permeant to anions other than chloride[22], we determined whether MOD-1 channels were also permeant to several anions. We measured the MOD-1 reversal potential in *Xenopus* oocytes, substituting chloride ions in the external medium with an equivalent concentration of six other anions of various sizes. The rank order of anion permeability for MOD-1 channels was thiocyanate ($E_{rev} < -40$ mV) > bromide ≈ iodide > chloride ($E_{rev} \approx -20$ mV) ≫ fluoride > aspartate ≫ gluconate ($E_{rev} > +50$ mV) (data not shown). This order is in agreement with the rank order for GABA- and glycine-gated chloride channels[22], indicating that the permeation properties of the MOD-1 channel are similar to those of GABA- and glycine-gated chloride channels.

We generated a green fluorescent protein (GFP) reporter of *mod-1* by inserting the *gfp* gene[23] into the *mod-1* minimal genomic rescuing fragment between the M3 and M4 domains (Fig. 2a). Stable chromosomally integrated lines of this construct[24] were rescued for the *mod-1* mutant phenotype (data not shown). *mod-1::GFP* reporter expression was observed in the cell bodies and axons (the latter presumably as a consequence of reporter overexpression) of several neurons in the head, ventral cord and tail of the animal (data not shown). No reporter expression was observed in any muscle cells. These observations indicate that the MOD-1 5-HT-gated chloride channel probably functions in neurons in *C. elegans*.

Voltage-clamp recordings from isolated embryonic Retzius cells from the medicinal leech *Hirudo medicinalis* indicate that 5-HT applications can result in hyperpolarizing chloride currents[25]. Recordings from dialysed whole cells and outside-out patches from these Retzius cells suggest that the 5-HT-gated chloride current is a consequence of a direct gating of a channel rather than the output of an indirect mechanism requiring second messenger cascades[26]. Our molecular identification and characterization of MOD-1 support this conjecture and demonstrate directly the existence of a 5-HT-gated chloride channel. We show that this channel acts as a 5-HT receptor *in vivo* and that its function is necessary for a 5-HT-mediated experience-dependent modulation of behaviour. If mammalian counterparts of MOD-1 exist, their identification and characterization might provide insights concerning the myriad neurobiological effects of 5-HT and define new targets for the development of human pharmaceuticals. □

Methods

Mapping and cloning of *mod-1*

We mapped *mod-1* using standard procedures[27] (see Supplementary Information). We performed germline transformation experiments[28] by injecting the various constructs along with 80 μg ml^{-1} pL15EK (which contains the wild-type *lin-15* gene) into a *mod-1(n3034); lin-15(n765ts)* strain and scoring stable transgenic lines, which produced non-Lin progeny. Rescued lines had at least half of the animals exhibiting normal sensitivity to 5-HT at 5 min in assays of 5-HT resistance.

Behavioural assays

Locomotory rate was assayed as described[3]. In Figs 1a and 3b, each trial involved testing at least five animals for each of the conditions; a given animal was tested for only one condition. *P* values were calculated by comparing the combined data for the mutants from all the separate trials to the combined data for the wild-type animals assayed in parallel for each condition of each separate trial. To assay 5-HT resistance, we placed 20 animals in 200 μl of 33 mM 5-HT (creatinine sulphate salt; Sigma) dissolved in M9 buffer[27] in 96-well microtitre wells and scored the swimming behaviour of such animals as active or immobile every minute for 20 min for the time-course experiments, at 5 min for germline transformation rescue experiments, or at 20 min (Fig. 3a). In this assay, an animal was scored as immobile if it did not exhibit any swimming motion for a period of 5 s.

Electrophysiological studies of MOD-1

An *Eco*RI/*Eco*RI fragment containing a full-length *mod-1* cDNA, including the 5′ and 3′ UTRs, was cloned into an *Eco*RI site of the vector pGEMHE[29] for oocyte expression and into the *Eco*RI site of vector GW1-CMV (British Biotech.) for transfection into HEK293 (ATCC # CRL-1533) cells. Capped cRNA for the oocytes was synthesized as described[29] and dissolved in water. RNA concentrations were determined by agarose gel electrophoresis and absorption spectroscopy. *Xenopus* oocytes were collected and injected with 50 nl RNA as described[29], and two-electrode voltage-clamp recordings were performed 1–3 days later at room temperature (22–25 °C) as described[29]. All compounds and wash solutions were applied to oocytes using a gravity-assisted perfusion system. The standard bath solution for the agonist, antagonist, and dose–response experiments was ND-96 (in mM): 96 NaCl, 2 KCl, 0.3 $CaCl_2$, 1 $MgCl_2$, 5 HEPES (pH 7.6). In Fig. 4b, each oocyte was sequentially subjected to 5-s treatments of increasing concentrations of 5-HT with 30 s of wash between applications. This protocol was continued from 10 nM to 1 μM, and then only one concentration higher than 1 μM was tested on any particular oocyte, as concentrations greater than 1 μM 5-HT led to desensitization and a decrease in the maximal response elicited by subsequent 5-HT applications. Responses from separate oocytes were combined by normalizing the amplitudes of each oocyte's responses to the various 5-HT concentrations to that elicited by 1 μM 5-HT. The normalized data were fit to the function $y = V_{max}[x^n/(k^n + x^n)]$ with a Hill coefficient (n) = 1, and then re-normalized to a maximal value of 1 by dividing by V_{max}. In Fig. 4c, 5-HT_{3a}-injected oocytes were first tested in buffer containing 0.3 mM Ca^{2+} and then 10 mM Ca^{2+}, as the 5-$HT3_a$-injected oocytes recovered very slowly from the 10 mM Ca^{2+} treatment. *mod-1*-injected oocytes were tested in both orders. The concentration of Ca^{2+} was varied in both the 5-HT and wash solutions. The 5-HT_{3a} traces were filtered digitally off-line at 5 Hz to reduce noise. In Fig. 4d and e, antagonists were present in both the 5-HT and wash solutions.

HEK293 cells were transiently transfected and whole-cell voltage-clamp recordings were done the next day as described[30]. Output was filtered at 10 kHz and sampled at 20 kHz using a Digidata 1200 interface. The patch pipette was coated with Sylgard, and the tip was heat polished to a final tip resistance in bath solution of 0.5–2 MΩ. The HEK293 cell was lifted from the dish with the recording pipette, and 5-HT was applied from a pressure-controlled spritzer pipette in the presence of a continuously flowing bath solution. The internal (patch pipette) solution contained (in mM): 130 potassium asparate, 10 KCl, 1 $MgCl_2$, 10 EGTA, 10 HEPES (pH 7.4). The external solution contained (in mM) 2 $CaCl_2$, 1 $MgCl_2$, 10 HEPES (pH 7.4), with varying proportions of sodium gluconate and NaCl, resulting in a final concentration of 140 mM of both Na^+ cations and gluconate plus Cl^- anions. Data analysis was performed off-line using Clampfit software (Axon), and curve fitting was accomplished using Origin (Microcal) or KaliedaGraph (Adelbeck) software.

Received 28 July; accepted 11 September 2000.

1. Martin, G. R., Eglen, R. M., Hamblin, M. W., Hoyer, D. & Yocca, F. The structure and signalling properties of 5-HT receptors: an endless diversity? *Trends Pharmacol. Sci.* **19,** 2–4 (1998).
2. Maricq, A. V., Peterson, A. S., Brake, A. J., Myers, R. M. & Julius, D. Primary structure and functional expression of the $5HT_3$ receptor, a serotonin-gated ion channel. *Science* **254,** 432–437 (1991).
3. Sawin, E. R., Ranganathan, R. & Horvitz, H. R. *C. elegans* locomotory rate is modulated by the environment through a dopaminergic pathway and by experience through a serotonergic pathway. *Neuron* **26,** 619–631 (2000).
4. Horvitz, H. R., Chalfie, M., Trent, C., Sulston, J. E. & Evans, P. D. Serotonin and octopamine in the nematode *Caenorhabditis elegans*. *Science* **216,** 1012–1014 (1982).
5. The *C. elegans* Sequencing Consortium. Genome sequence of the nematode *C. elegans*: a platform for investigating biology. *Science* **282,** 2012–2018 (1998).
6. Krause, M. & Hirsh, D. A trans-spliced leader sequence on actin mRNA in *C. elegans*. *Cell* **49,** 753–761 (1987).
7. Liu, L. X. *et al.* High-throughput isolation of *Caenorhabditis elegans* deletion mutants. *Genome Res.* **9,** 859–867 (1999).
8. Jansen, G., Hazendonk, E., Thijssen, K. L. & Plasterk, R. H. Reverse genetics by chemical mutagenesis in *Caenorhabditis elegans*. *Nature Genet.* **17,** 119–121 (1997).
9. Sumikawa, K. & Gehle, V. M. Assembly of mutant subunits of the nicotinic acetylcholine receptor lacking the conserved disulfide loop structure. *J. Biol. Chem.* **267,** 6286–6290 (1992).
10. Karlin, A. & Akabas, M. H. Toward a structural basis for the function of nicotinic acetylcholine receptors and their cousins. *Neuron* **15,** 1231–1244 (1995).
11. Cooper, J. R., Bloom, F. E. & Roth R. H. *The Biochemical Basis of Neuropharmacology* (Oxford Univ. Press, New York, 1996).
12. Hardie, R. C. A histamine-activated chloride channel involved in neurotransmission at a photoreceptor synapse. *Nature* **339,** 704–706 (1989).
13. McClintock, T. S. & Ache, B. W. Histamine directly gates a chloride channel in lobster olfactory receptor neurons. *Proc. Natl Acad. Sci. USA* **86,** 8137–8141 (1989).
14. Cully, D. F. *et al.* Cloning of an avermectin-sensitive glutamate-gated chloride channel from *Caenorhabditis elegans*. *Nature* **371,** 707–711 (1994).
15. Adelsberger, H., Lepier, A. & Dudel, J. Activation of rat recombinant $\alpha_1\beta_2\gamma_{2S}$ $GABA_A$ receptor by the insecticide ivermectin. *Eur. J. Pharmacol.* **394,** 163–170 (2000).
16. Krause, R. M. *et al.* Ivermectin: a positive allosteric effector of the α7 neuronal nicotinic acetylcholine receptor. *Mol. Pharmacol.* **53,** 283–294 (1998).
17. Davies, P. A. *et al.* The 5-HT_{3B} subunit is a major determinant of serotonin-receptor function. *Nature* **397,** 359–363 (1999).
18. Downie, D. L. *et al.* Pharmacological characterization of the apparent splice variants of the murine 5-HT_3 R-A subunit expressed in *Xenopus laevis* oocytes. *Neuropharmacology* **33,** 473–482 (1994).
19. Aizenberg, D. *et al.* Mianserin, a 5-HT2a/2c and alpha 2 antagonist, in the treatment of sexual dysfunction induced by serotonin reuptake inhibitors. *Clin. Neuropharmacol.* **20,** 210–214 (1997).
20. Granas, C. & Larhammar, D. Identification of an amino acid residue important for binding of methiothepin and sumatriptan to the human 5-HT(1B) receptor. *Eur. J. Pharmacol.* **380,** 171–181 (1999).
21. Weber, W. Ion currents of *Xenopus laevis* oocytes: state of the art. *Biochim. Biophys. Acta.* **1421,** 213–233 (1999).
22. Bormann, J., Hamill, O. P. & Sakmann, B. Mechanism of anion permeation through channels gated by glycine and gamma-aminobutyric acid in mouse cultured spinal neurones. *J. Physiol. (Lond.)* **385,** 243–286 (1987).
23. Chalfie, M., Tu, Y., Euskirchen, G., Ward, W. W. & Prasher, D. C. Green fluorescent protein as a marker for gene expression. *Science* **263,** 802–805 (1994).
24. Shaham, S. & Horvitz, H. R. Developing *Caenorhabditis elegans* neurons may contain both cell-death protecture and killer activities. *Genes Dev.* **10,** 578–591 (1996).
25. Lessmann, V. & Dietzel, I. D. Development of serotonin-induced ion currents in identified embryonic Retzius cells from the medicinal leech (*Hirudo medicinalis*). *J. Neurosci.* **11,** 800–809 (1991).
26. Lessmann, V. & Dietzel, I. D. Two kinetically distinct 5-hydroxytryptamine-activated Cl^- conductances at Retzius P-cell synapses of the medicinal leech. *J. Neurosci.* **15,** 1496–1505 (1995).

27. Brenner, S. The genetics of *Caenorhabditis elegans*. *Genetics* **77,** 71–94 (1974).
28. Mello, C. C., Kramer, J. M., Stinchcomb, D. & Ambros, V. Efficient gene transfer in *C. elegans*: extrachromosomal maintenance and integration of transforming sequences. *EMBO J.* **10,** 3959–3970 (1991).
29. Morrill, J. A. & Cannon, S. C. Effects of mutations causing hypokalaemic periodic paralysis on the skeletal muscle L-type Ca^{2+} channel expressed in *Xenopus laevis* oocytes. *J. Physiol. (Lond.)* **520,** 321–336 (1999).
30. Hayward, L. J., Brown, R. H. Jr & Cannon, S. C. Inactivation defects caused by myotonia-associated mutations in the sodium channel III-IV linker. *J. Gen. Physiol.* **107,** 559–576 (1996).

Supplementary information is available on *Nature*'s World-Wide Web site (http://www.nature.com) or as paper copy from the London editorial office of *Nature*.

Acknowledgements

We thank N. Buttner, D. Omura and P. Reddien for suggestions concerning this manuscript; G. Moulder and R. Barstead for help in isolating the *mod-1(ok103)* allele; L. Liu and C. Johnson for sharing the *mod-1(nr2043)* allele before publication; and D. Julius for the 5-HT_{3a} cDNA clone. This work was supported by a grant from the United States Public Health Service (H.R.H.). R.R. is supported by a Howard Hughes Medical Institute predoctoral fellowship. H.R.H. is an Investigator of the Howard Hughes Medical Institute.

Correspondence and requests for materials should be addressed to H.R.H. (e-mail: horvitz@mit.edu). The nucleotide sequence of the *mod-1* cDNA has been deposited at GenBank under the accession number AF303088.

Notch signalling and the synchronization of the somite segmentation clock

Yun-Jin Jiang*, Birgit L. Aerne†, Lucy Smithers*‡, Catherine Haddon*, David Ish-Horowicz† & Julian Lewis*

* *Vertebrate Development Laboratory and* † *Developmental Genetics Laboratory, Imperial Cancer Research Fund, 44 Lincoln's Inn Fields, London WC2A 3PX, UK*

In vertebrates with mutations in the Notch cell–cell communication pathway, segmentation fails: the boundaries demarcating somites, the segments of the embryonic body axis, are absent or irregular[1–8]. This phenotype has prompted many investigations, but the role of Notch signalling in somitogenesis remains mysterious[1,9–12]. Somite patterning is thought to be governed by a "clock-and-wavefront" mechanism[13]: a biochemical oscillator (the segmentation clock) operates in the cells of the presomitic mesoderm, the immature tissue from which the somites are sequentially produced, and a wavefront of maturation sweeps back through this tissue, arresting oscillation and initiating somite differentiation[14,15]. Cells arrested in different phases of their cycle express different genes, defining the spatially periodic pattern of somites and controlling the physical process of segmentation[1,16–19]. Notch signalling, one might think, must be necessary for oscillation, or to organize subsequent events that create the somite boundaries. Here we analyse a set of zebrafish mutants and arrive at a different interpretation: the essential function of Notch signalling in somite segmentation is to keep the oscillations of neighbouring presomitic mesoderm cells synchronized.

We have analysed the expression patterns of two zebrafish *Delta* homologues, *deltaC* and *deltaD*[10,20,21]. These code for Notch ligands, and their patterns reveal both the existence of a segmentation clock in the zebrafish and its linkage to the Notch pathway. Expression of *deltaC* marks the posterior part of each formed somite; expression of *deltaD* marks the antero-medial part[20]. Meanwhile, expression in the presomitic mesoderm (PSM) appears to be dynamic. In a batch of sibling embryos all fixed at the same time, a variety of stripy PSM expression patterns of *deltaC* and *deltaD* are seen. This variation is most obvious for *deltaC*. The expression patterns can be arranged tentatively as phases of a cycle (Fig. 1), resembling the cycle of patterns of *c-hairy1* expression in the chick embryo[14]. Following the chick convention[14], we divide the cycle of patterns into three intervals, labelled phases I, II and III. Embryos at different ages show the same range of patterns, with similar relative frequencies (315 embryos scored, stages from 1 to 10 somites), as expected for a repetitive cycle.

To prove that the different *deltaC* expression patterns represent consecutive states of a cyclic process, we analysed embryos developing in a temperature gradient that causes somitogenesis to go faster on one side of the body than on the other. Embryos at the 5–10-somite stage were placed on their sides in a chamber with a warm floor and a cool ceiling, giving a temperature gradient calculated to cause the rate of somitogenesis to be faster on the warm side of the body than on the cold side by 0.2–0.3 somites per hour (see Methods). We took batches of embryos that had been exposed to the temperature gradient for the same fixed time (1.5 h, corresponding to a left–right difference of 0.3–0.45 of a somite cycle) and compared the patterns of *deltaC* expression between the two sides (Fig. 2). Typically, when the cool side showed a phase I pattern (as defined in Fig. 1), the warm side showed a phase II pattern; when the cool side showed a phase II pattern, the warm side showed a phase III pattern; and when the cool side showed a phase III pattern, the warm side showed a phase I pattern (see Fig. 2 for details). The phases therefore succeed each other cyclically. Long periods in the temperature gradient caused more extreme differences between the two sides, and after 3.5 h embryos could be seen in which the warm side was once again in the same phase as the cool side, but with one extra somite (Fig. 2d).

The stripes of expression seen in the PSM correspond to repeated waves of *deltaC* expression, sweeping through a much more slowly moving cell population (see Supplementary Information). Like the *c-hairy1* waves in the chick[14], these 'kinematic waves' are the sign of an intracellular oscillation that slows down, changes its amplitude and finally comes to a halt as cells progress from the posterior PSM to the anterior PSM and emerge into the region where somite boundaries finally become determined (see ref. 14 for analysis). The clock-and-wavefront mechanism therefore appears to be a fundamental feature of vertebrate somitogenesis, conserved from fish to birds and mammals.

Using the expression of *deltaC* as an indicator, we examined how oscillator behaviour is altered in the somitogenesis mutants *beamter* (*bea*), *deadly seven* (*des*), *after eight* (*aei*) and *mind bomb* (*mib*)[22–24]. These all have a somite phenotype like that of Notch pathway mutants in the mouse: somite boundaries fail to form correctly, except for the first 5–8 (the most anterior), which appear normal. The *mib* mutation makes cells deaf to Notch signalling in other tissues[23,25], *aei* corresponds to *deltaD*[26] and *des* shows neurogenic abnormalities in the neural plate similar to those of *mib* but weaker (data not shown). Thus we can ascribe the somite phenotype in fish, as in mouse, to a defect in Notch signalling.

Figure 3 shows the *deltaC* expression pattern for each of the four mutants at the 10-somite stage. The expression pattern is the same in each case, and abnormal in four respects. First, all mutant embryos in a batch show the same pattern, with moderate levels of expression in the posterior part of the PSM, relatively low levels in the middle part, and high levels in the anterior part. Second, in the anterior PSM, the two strong stripes visible in most phases of the normal cycle are replaced by a single abnormally broad stripe. Third, levels of expression are abnormally variable from cell to cell; this is particularly obvious in the anterior PSM, where there is a random mixture of strongly and weakly expressing cells instead of the usual alternating stripes of very high and very low expression

‡ Present address: Gene Function and Regulation, Institute of Cancer Research, Chester Beatty Labs, Fulham Road, London SW3 6JB, UK.